2022 IEEE 18th International Conference on Automation
Science and Engineering (CASE)
August 20-24, 2022. Mexico City, Mexico

Robotic Fabric Fusing using a Novel Electroadhesion Gripper

Honglu He, Glenn Saunders, John T. Wen

Abstract— **Automation has been playing a major role in manufacturing such as in automotive, electronics, and pharmaceutical industries. While robots are able to perform repeatable tasks with speed and accuracy, its use in garment industry has been limited by challenges in grasping and handling soft fabrics using commercially available robot end effectors. This paper considers a common garment manufacturing process, *fabric fusing*, which combines a piece of woven or knitted fabric with an interface material (interlining) to provide additional firmness and support. Current practice uses human operators to perform fabric pick-up, alignment, and manipulation tasks to feed the combined materials into a fusing machine. We have developed a robotic system with an electroadhesion robot gripper containing actuated pins to alleviate human operators from performing these repeated and laborious tasks in an uncomfortable manufacturing environment. This robotic system can reliably pick-up fabric pieces, place them without wrinkles, align them using machine vision, and feed the combined bundle through the conveyor belt into the fusing machine. The actuated pins interlaced with the electrodes on the gripper can detach the fabric from the gripper with residual charges and to slide the bundle onto the conveyor belt without affecting the fabric alignment. The electroadhesion force depends on the applied voltage, fabric material property, and humidity. The environmental condition needs to be controlled and the applied voltage adjusted based on the type of fabric materials and humidity to achieve reliable performance. The prototype system has been demonstrated in both the laboratory setting and actual garment manufacturing shop floor.**

***Keywords*- Electroadhesion, Fabric Fusing, Garment Manufacturing, Robot Gripper**

I. INTRODUCTION

Robots are now commonly used in factories across different industries such as automotive, aerospace, electronics, and chemical manufacturing [1]–[4]. They help to reduce manual labor drudgery while increasing productivity and repeatability. While robots are able to perform complicated tasks in large scale and with heavy load, they are most successful in highly structured environment where robots perform repeated tasks. Garment industry presents a different set of challenges. Soft and threaded fabric materials are difficult to pick up reliably using common robotic grippers and it is challenging to place them accurately and without winkles. As a result, garment industry, while gaining automation through in fabric processing such as cutting, sewing, welding, etc., handling fabrics to present them to these automation machineries is still largely manual. For example, human operators often need to utilize both hands and multiple fingers to separate a single layer from a pile and place it accurately and flatly without wrinkles as shown in Fig. 1.

Fig. 1: Manual preparation of fabric bundles for the fusing machine involves aligning and stacking interlining fabric on top of the shell fabric.

There have been special grippers designed for fabric handling [5]–[10]. A review of grippers for fabric pick-up is given in [11]. These gripper designs have specific domain of applicability and offer trade-offs in performance and reliability. Parallel gripper design shows good manipulablity of fabric, but may not be suitable for picking up single pile from a stack directly [5]. Soft gripper with microneedles shows good performance on single sheet separation for different fabric types, but a single point of contact with the fabric may not have enough manipulability for fusing/sewing purposes [6]–[8]. Roller based gripper also does a good job in fabric separation, but may not work well for ultra thin fabric like interlining [9], [10]. Suction grippers are not able to pick up fabrics due to porosity, and often needed to combine with air-jet and clamps; adhesive type of gripper requires constant replenishment to maintain the same amount of adhesive force. Small-nail/saw-tooth type of gripper may damage more fragile fabrics [11].

Electroadhesion is an adhesion force caused by high voltage electrostatic effect. Basic electroadhesion properties and modeling have been well studied [12] and have been proposed for fabric handling [13], [14]. Several implementations use small surface contact rollers to hold parts of the fabric rather than the entire fabric [13]. Electroadhesion plate has been used for flat fabric pick-up in [15], [16] but the focus is on the pick-up force rather than both pick-up and release. Flat electrostatic gripper has been patented and commercialized by Grabit Inc. [17], including modular electrode design [18] and pogo pins between electrodes for fabric release [19]. While this technology, as well as other

Electrical, Computer, and Systems Engineering, Rensselaer Polytechnic Institute, heh6@rpi.edu
Manufacturing Innovations Center, Rensselaer Polytechnic Institute, saundg@rpi.edu
Electrical, Computer, and Systems Engineering, Rensselaer Polytechnic Institute, wenj@rpi.edu

proposed robotic fabric grippers mentioned above, may be able to handle a single ply efficiently, they have not been shown to perform consistently in tasks such as ply separation, translation, and alignment. Further, though the impact of environmental conditions, such as surface condition and humidity, on electrostatic force has been considered in the past, [20], there has not been automatic adjustment algorithm for the applied voltage to the electrode to account for the changing environmental condition.

In this paper, we consider a specific garment manufacturing process called fabric fusing which combines a piece of fabric with an interface material for reinforcement. This process involves a human operator picking up each piece of fabric, aligns and places one on top of the other, and feeds the combined bundle onto a conveyor belt into a fabric fusing machine. We have developed a prototype robotic system including an electroadhesive fabric gripper and camera-based vision sensing to perform the fabric fusing operation autonomously. The system can take fabric information from the operator, pick up a single piece from the pile at a time, align and place the pieces without wrinkles, and manipulate the combined bundle securely onto the conveyor belt for fusing. This paper presents the overall robotic system architecture, the design of the electroadhesion fabric gripper to balance between the adhesion force and depth of penetration, and the performance for different types of fabrics and interlinings. Key aspects of the system includes:

- Electroadhesion plate manufacturing: The manufacturing process is cost-effective, involving multilayer PCBs to mount on the electrostatic plate and a rigid acrylic gripper structure.
- Fabric manipulation: The spring-loaded pins securely press down on the fabric bundle to ensure the integrity (wrinkle-free alignment) of the bundle.
- Single ply fabric pick-up from a fabric pile: This is achieved through careful electrode design (balance between pick-up force and depth of electric field penetration) and appropriate levels of applied voltage.
- Electromechanical fabric placement: The fabric is released from the gripper without introducing wrinkles by combining the actuated pins and charge removal.
- Vision-guided operation: Machine vision on the robot wrist is used to orient the gripper to ensure complete coverage of the fabric by the gripper. Machine vision in the workspace is used to ensure alignment between the fabric and interlining.
- Adjustment for environmental condition: Humidity and applied voltage need to be adjusted based on the type of fabric to ensure consistent result.

The system has been tested in the laboratory setting as well as on the actual garment manufacturing shop floor. Out of the six different types of fabrics, we have identified the working range of humidity for five of them that can achieve over 80% success rate in terms of fabric pick-up. Once the fabric is successfully picked up, the remaining process works reliably.

II. Fabric Fusing and Electroadhesion Background

Fabric fusing is a process that joins two different types of fabric together: shell fabric and interlining fabric (interface material). Shell fabric is usually heavier, as an outer layer of clothing; interlining fabric is a fabric attached to the shell fabric as the inner layer, which is usually coated with adhesive resin [21]. During the fusing process, the interlining fabric is aligned and placed on top of the shell fabric and the combined bundle is fed into the fusing machine. While the fusing machine presses down and heats up the combination, the interlining surface becomes adhesive and affixes to the shell fabric. Fig. 2 shows sample pieces from our testbed: green parts are interlining fabric and gray parts are shell fabric. At the top, the two blue bins contain shell and interlining fabrics. One piece from each bin is placed on the assembly station to form the combined bundle and fed into the fusing machine through conveyor belt.

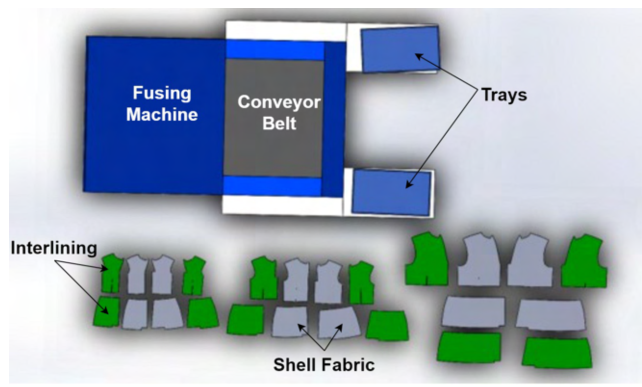

Fig. 2: Fusing Process Schematics. Green pieces are interlining fabric. Gray pieces are shell fabric. Blue bins are fabric containers, one for the interlining fabric and one for the shell fabric. The blue square depicts the fusing machine. The grey area in front of the fusing machine consists of a conveyor belt and an assembly area for the fusing bundle.

The electroadhesion phenomenon was discovered in early 1900's. It has been applied in robotics applications such as wall-climbing robots and soft robotic grippers [22], [23]. The underline principle in electroadhesion is electrostatic force, but the mechanism differs between conductive and insulated substrate materials. For conductive materials, electroadhesion force is generated through charge induction of free electrons within the material. For insulated materials, electroadhesion force is dominated by dielectric polarization [24], [25]. Electroadhesion plates are either unipolar or bipolar, corresponding to a single pole or double poles, respectively. Bipolar designs generally exert larger amount of adhesion force than the unipolar design, especially on insulated materials [26]. However the calculation of the force has remained inexact due to the influence of multiple factors such as dielectrics and material substrates properties and environmental conditions.

The advantage of picking up fabric with an electroadhesion gripper is that a large piece of fabric could be picked securely on the plate and placed without wrinkles while maintaining full manipulability. But there also challenges such as how to generate enough adhesion force for different materials, how to dissipate remaining charge for placement, and how to avoid picking multiple layers [27].

III. Fabric-Specific Electroadhesion Design

In this research study, we choose the bipolar inter-digital design for the larger adhesion force. To achieve high voltage, a 5 V DC to 10 kV DC converter is connected to the output of analog voltage source as the analog adhesion force control unit. We use the ADALM1000 evaluation board by Analog Devices Inc., henceforth referred to as the M1K board, as the voltage source [28].

For testing, we use 3 types of interlining fabric and 4 types of shell fabric (fabric name: weight per square meter, material, thickness per layer, (I) for interlining):

- Army Khaki: 339 g, 55% Polyester, 45% Wool, 0.5 mm
- Army Green: 407 g, 55% Polyester, 45% Wool, 0.5 mm
- Suit Fabric: 305 g, 100% Wool, 0.25 mm
- Postal Fabric: 407 g, 100% Polyester, 0.33 mm
- Army Black: 100 g, 100% Polyester, 0.28 mm (I)
- Polo Grey: 70 g, 100% Polyester, 0.25 mm (I)
- Light Black: 30 g, 100% Polyester, 0.15 mm (I)

For each material there are 5 shapes (upper left, upper right, lower left, lower right and collar) and 3 sizes (36, 44 and 56) as jacket front parts.

A. Initial Tests

In past research, electroadhesion plates are made through the customized etching or jet printing processes [25], [29]. Our goal is to develop the gripper fabrication process accessible, repeatable and cost efficient. The development went through several phases:

- **Proof of Concept**: We made a quick initial prototype from aluminum foil and saran wrap to verify the feasibility of using electroadhesion to manually pick up a large piece of fabric. This first, though crude, is able to pick up the light weight interlining fabric but not any of the shell fabric.
- **Design Iteration #2**: The goal of the next design iteration is to make an electroadhesion plate with larger adhesion force and attachable to the robot end plate. This version is made of aluminum foil and two thin acrylic plates. The top plate is attached to the robot end-effector. This version is able to grip the fabric, but unable to release the fabric when the high voltage is shut off. This is because of the plate acting like a capacitor, the residual charges can hold the fabric well even after the voltage supply is off. Moreover, due to its large size, the whole electroadhesion plate tends to warp. This suggests the need for a support structure and a high voltage relay for discharging.
- **Design Iteration #3**: The next design iteration includes a support structure with two layers. The bottom layer is the electroadhesion plate (two thin acrylic plates and aluminum foil electrodes), and the upper layer is a plate with pins connected to a pneumatic actuator to help with the fabric release. The mechanical structure is shown in Fig. 3. The electric connection, including a high voltage relay, is as shown in Fig. 4. R1, R2 and R3 are 15 $M\Omega$ resistors to prevent high voltage electric impulses. The high voltage relay and the valve are controlled by robot controller digital I/O, while the M1K board is controlled by a laptop computer.

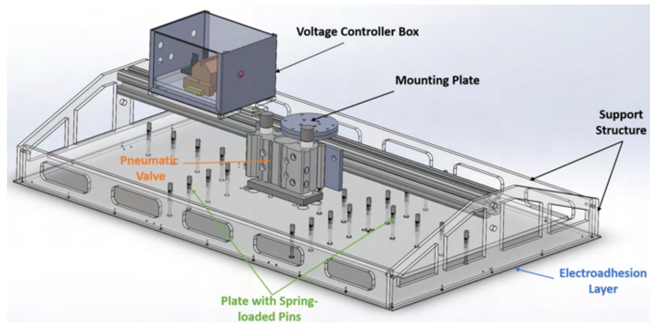

Fig. 3: Gripper Structure Design.

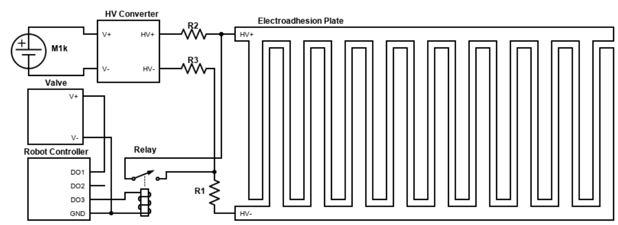

Fig. 4: Electroadhesion Electrical Circuit Diagram. Connections from robot controller are 24 V digital I/O and from M1k analog is 5 V output.

With the ability to control the electroadhesion charging and discharging process, we can experiment with pick and place tests using the robot. The test procedure is described as below:

Step 1: Jog to home configuration.
Step 2: Jog to the top layer of the fabric.
Step 3: Turn on voltage control to 6 kV.
Step 4: Wait 1 s for the gripper to be fully charged.
Step 5: Jog to the place station.
Step 6: Turn off voltage control and turn on relay.
Step 7: Actuate pins to push fabric down against residual charges.

The pick and place test is repeated for all types of fabric, but the gripper is only able to pick up and release interlining fabric. For heavier shell fabric, the elecoradhesion plate only manages to partially pick up the fabric instead of the entire piece. Increasing the applied voltage may help with the adhesion force, but causes electric arcs between aluminum traces. The conclusion is that to allow higher voltage on the electroadhesion plate, it is necessary to use a different dielectric material

(a) PCB Sample

(b) Acrylic Casting

Fig. 5: PCB samples and acrylic casting considered for in design iterations to increase the adhesion force.

rather than air.

- **Design Iteration #4**: In order to embed the electrodes into a dielectric material for large sizes, we tried two approaches: liquid acrylic casting and custom PCB samples with inter-digital copper traces, shown in Fig. 5. Liquid acrylic casting failed because it is hard to control the thickness due to the high viscosity. The PCB samples have two copper layers, with the top layer containing interdigital copper traces and an empty bottom layer. Each PCB sample has 7 mm trace width and 4 mm gap between traces. When applying 8 kV across the electrodes, electric arc occurs again above the top layer through air. This is due to the fact the two-layer PCB contains copper layers not fully embedded within the dielectric. This design is encouraging in that even a small PCB sample is able to pick up the heavier shell fabric. However, it is not possible to manufacture a PCB of size 0.8 m $\times$ 0.5 m required for our fabric samples.
- **Final Design**: The final electroadhesion plate is designed to be a thin acrylic plate with six 4-layer PCB panels attached. The detailed design of this final version is described in the next section.

B. PCB Design Optimization

Throughout the tests with small PCB samples, it is noticeable that for interlining fabric, the electroadhesion gripper may pick up multiple layers. To guide the design of the electrode geometry, we use the MATLAB PDE toolbox to evaluate the electric field between the traces [30]. Simulation results shown in Fig. 6 indicate that a design with a smaller gap between traces tends to produce stronger electric field closer to the electrodes, and the gradient along the z-axis (vertical to the plate) is much sharper than the larger gap design. This implies that a smaller gap would result in smaller electroadhesion force on the fabric at the second layer, hence avoiding picking up multiple layers. According to the results in [25], the optimal width/gap ratio is 1.8, so our PCB is designed with trace width 1.8 mm and gap width 1 mm [25].

C. Releasing and Sliding Mechanism

This gripper is not only designed to pick up and place a single layer of fabric, but also align the fabric pieces accurately and feed the combined bundle onto a conveyor

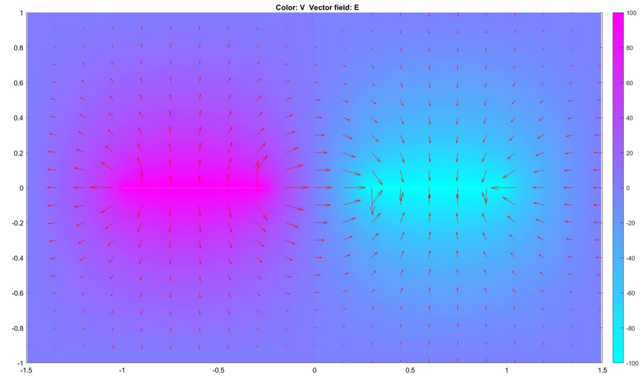

(a) PDE Visualization

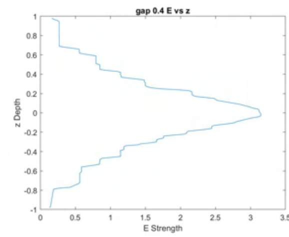

(b) electric field vs. distance (larger gap)

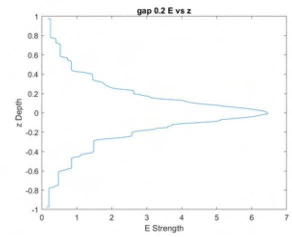

(c) electric field vs. distance (smaller gap)

Fig. 6: MATLAB PDE Simulation with Larger and Smaller Gap for Two Thin Electrodes with Unit Charge and Vacuum Permittivity. a) is the plotted solutions, where the arrow represents the direction of electric field and its length is the electric field strength. b) and c) are the electric field strength along the plate normal direction between two electrodes. This is proof of concept of relationship between separation distance and electric field strength.

belt. The pneumatically-actuated pins between PCB's serve the purposes for fabric releasing and manipulating on a flat surface. During the fabric placement process, the electroadhesion plate is turned off, while remaining residual charges may still hold the fabric tight. The pins are then actuated to push fabric off the electroadhesion plate onto the station. These pins are also useful to slide the fabric bundle without causing wrinkles and fabric misalignment onto the conveyor belt. To ensure secure engagement between the gripper and the fabric under slight misalignment between the gripper surface and the fabric, we added passive compliance through spring-loaded pins. At the tip of each pin, there is also a cross pattern crafted to increase the friction between the pin and fabric, as shown in Fig. 7a. The numbers and distribution of the pins is determined through the residual force of electroadhesion after the voltage is off. Since each pin requires a hole on the bottom plate to travel through, it's necessary to keep minimum number of pins and align them together in several straight lines to allow minimum separation distances PCB's to achieve maximum electroadhesion force.

The final gripper is shown as Fig. 7b.

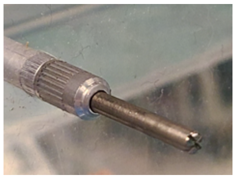

(a) Spring-loaded pin

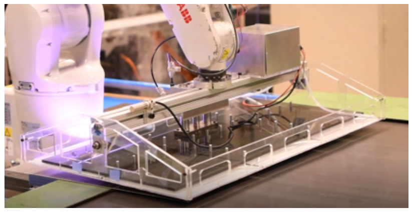

(b) Final gripper outcome

Fig. 7: Final Gripper Design. a) Spring-loaded pin with cross pattern at the tip; b) Assembled gripper mounted at the robot end-effector with all connections.

IV. Software Architecture

Our prototype system uses an ABB IRB 1200 industrial robot. The IRB robot series offers an optional External Guided Motion (EGM) interface allowing direct joint position command streaming at 250 Hz. While most parts of the robot motion in this research study simply jogs to the pre-taught waypoints, visual servoing in section VI-C takes advantage of EGM to achieve fabric alignment.

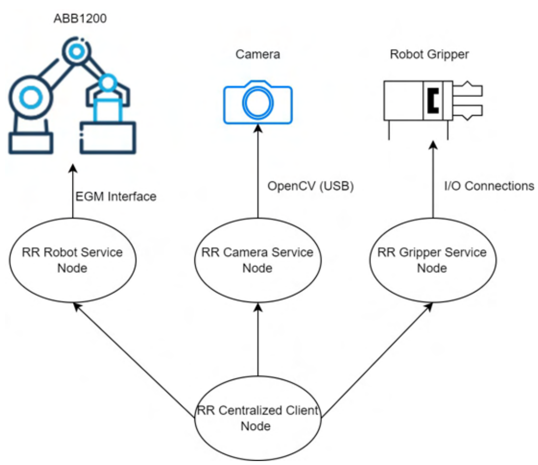

Fig. 8: RR Node Connection Diagram. Each service node exposes its object over the network, and one centralized client node talks to all services.

For integration between different components, we use Robot Raconteur (RR) as our robotic middleware [31], [32]. Robot Raconteur is a communication library, which exposes nodes over the local network. For each hardware component: robot, gripper and camera, there is a designated RR service containing a program object. For the final operation, there is a client node connecting to all service objects, commands and receives real time data as shown in Fig. 8.

V. Testbed Development and Performance Evaluation

According to previous research studies, electroadhesion is prone to humidity changes [25]. In order to maintain the desired humidity, an enclosed chamber is built around the robotic fusing work cell. Most of our experiments have been conducted in winter; the ambient relative humidity is below 30%, so humidifiers are needed to maintain consistent performance. There is a humidity sensor installed at the edge of fabric load bin, which provides humidity reading near the fabric. From initial tests, we noticed that the humidity inside the chamber is not uniform due to humidifiers, so fans are installed within the testbed to help circulating the air to achieve a uniform humidity. In our lab, we also have an fusing machine with a conveyor belt, similar to the setup in actual garment factories.

The complete robotic fusing testbed includes:

- Two tables holding the fabric bins (one for interlining and one for shell fabrics).
- Humidifiers
- Air circulating system
- Placing plate (for fabric bundle assembly) with a camera
- ABB IRB 1200 robot
- Acrylic Enclosure
- Humidity Sensors ($\pm 2\%$ accuracy)

This testbed is easily assembled/dissembled for transportation to different sites. The testbed in our lab is shown in Fig. 9.

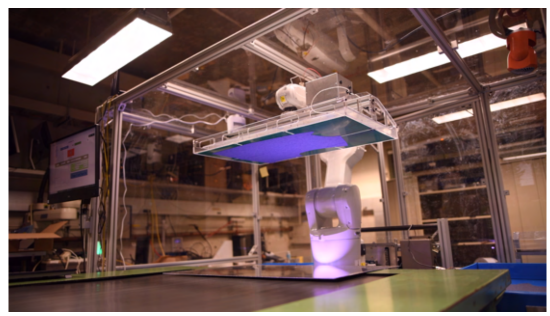

Fig. 9: Final Testbed Setup. The monitor is the user interface. Two fans at the ceiling helps circulating the air inside the chamber. Humidifiers are underneath. Fabric trays are loaded on both sides of the robot.

A. *Effect of Humidity*

Because each fabric type has its unique material property, we first determine which types of fabric are suitable for electroadhesion. According to electroadhesion studies, electroadhesion force increases monotonically with respect to the applied voltage across electrodes, in a nonlinear relationship [33], [34]. Hence, for testing each type of fabric, the voltage is tuned to be the minimum that can pick up a single layer reliably. Each pile contains ten layers of fabric, and the humidity is measured next to the fabric. Due to long signal wire along the robot arm to high voltage converter, there is a voltage loss, and the maximum output voltage to the electroadhesion plate is 9 kV. In the tests, size 44 and shape lower left is used for all types of fabric.

From the result shown in Table I, we learned that electroadhesion is able to pick up most types of fabric, but different fabric has different humidity range. More importantly, for Light Black interlining material, our electroadhesion gripper may be able to separate a single layer from a bundle at certain

RH(%)	30	40	50	60
Light Black	6.3(6/10)	5.4(8/10)	3.8(8/10)	3.8(10/10)
Polo Grey	9(10/10)	9(10/10)	9(10/10)	9(4/10)
Army Black	9(10/10)	9(10/10)	9(10/10)	9(4/10)
Army Green	9(0/10)	9(0/10)	9(8/10)	9(10/10)
Army Khaki	9(0/10)	9(0/10)	9(6/10)	9(5/10)
Suiting	9(0/10)	9(7/10)	9(8/10)	9(5/10)
Postal	9(8/10)	9(7/10)	9(4/10)	9(0/10)

TABLE I: Humidity and Fabric Performance: Applied Voltage(kV) (Successful Rate: picking up a single layer from a bundle)

humidity, but will not pick up "cleanly": the second or even third layer may get adhered/entangled at first, but falls off as the gripper moving up with large wrinkles. This problem also shows up occasionally for thin fabrics such as suiting and postal fabric and other interlinings depending on the applied voltage, but never for poly-wool shell fabric (Army Green / Army Black).

To find the best humidity range for all types of fabric, we decided to apply the maximum voltage on the electroadhesion gripper and run the test again at different humidity. Here the successful picking up is defined as picking up a single layer without interfering following layers. The result is shown in Fig. 10, indicating that the best humidity at around 50%.

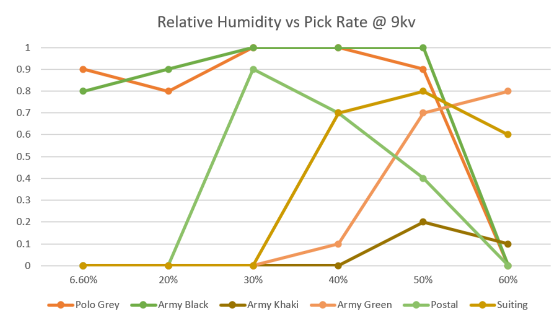

Fig. 10: Pick-up Success Rate vs. Humidity. Interlining fabric tends to have a lower working humidity range with electroadhesion than shell fabric. There is an optimal humidity at around 50% where all fabric is able to be picked up.

Since electroadhesion generates force per unit area [35], under the same environment the gripper has similar performance with different shapes and sizes as long as the gripper covers the whole fabric. However, due to the nature of fabric, if fabric threads are entangled together along the edges, the gripper will likely fail to pick up the fabric. This issue is noticeable for upper parts, which include a split in the middle as shown in Fig. 11.

VI. Fusing Fabric Alignment with Visual Servoing

We apply vision-guided robot motion to perform fabric alignment. With the camera pointing upward from the placing station, it has a full view of the entire electroadhesion plate. Due to the size of the gripper, the orientation of fabric within each bin is pre-determined, meaning that the operator has to load fabric into the right orientation, such that the robot could avoid a 180° end-effector rotation motion.

Fig. 11: Upper right fabric with a split in the middle, where threads are likely to be entangled.

A. Calibration

Since the goal is to align two fabric pieces instead of placing them into an exact pre-defined location, there is only the relative accuracy requirement and no need for a world coordinate system. The initial calibration includes:

1) Find the robot configuration to allow the camera to determine the fabric configuration. Call this configuration the fabric inspection configuration.
2) Determine the pixel area to physical area ratio.

Since the camera is mounted with its z-axis (optical axis) pointing upward, the fabric inspection configuration must have the robot end-effector z-axis pointing downward. The fabric inspection configuration is determined to ensure the plate is completely within the camera field of view (FOV) as well as to identify the region of interest (ROI) where the plate lies.

Given the CAD file of each fabric like Fig. 12, it is necessary to extract the template image with correct pixel sizes. Hence this ratio could be determined from the pixel area of ROI divided by the actual area of the elctroadhesion plate.

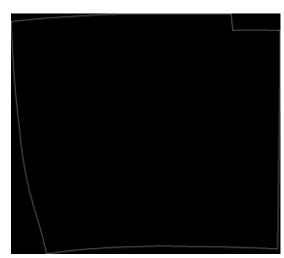

Fig. 12: Lower left size 36 template, extracted from fabric CAD file.

B. Template Matching

Template matching is the simplest way to identify a known pattern within an image. The generic template matching method is to run the edge detection first and then use the sum of square difference (SSD) to detect the location of desired pattern [36], [37]. However, in our case, the edge detection may return noisy results due to the PCB inter-digital design. Hence, by making all edges bolder, the filtered image is left with center part with fabric almost black (edge-free) while all white (edges) outside, resulting in a much more robust detection. Moreover, if the gripper fails to pick up the fabric, the overall SSD will be much larger than when there is fabric. This allows the determination on whether the gripper picks up the fabric or not by setting a minimum SSD error threshold.

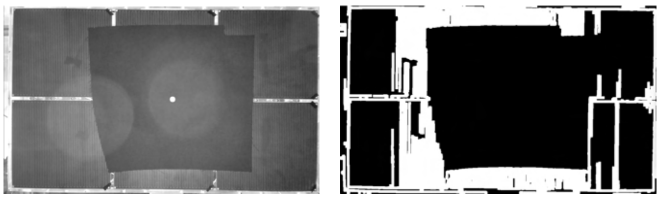

(a) Original Image (b) Edge Filtered Image (Bold)

Fig. 13: Template Matching Result: a) is the original image with identified fabric centroid; b) is the output from edge detection with all bolder edges.

To determine the template orientation in the image, within a certain orientation range, the template is rotated to different angles to produce different orientation templates. By checking each orientation templates with template matching, the minimum sum of square difference returns the best angle and pixel coordinates.

In cases when the gripper fails to pick up the fabric, the filtered image with bold edges will return a large number in sum of square difference, which could classified as fabric not found. Fig. 13 shows the example output from the template matching algorithm.

C. Visual Servoing

Since the fabric is already loaded in a known direction, the template matching algorithm runs initially within $\pm 10°$ range and $1°$ resolution. After finding the best image coordinates and angle, the algorithm runs again within $\pm 1°$ range and $0.1°$ resolution. After the position and orientation are determined, the robot brings the template centroid to the center of ROI with continuous fixed-orientation template matching feedback. Then the robot will place the fabric to a predefined place position plus the recorded offset position and orientation. Fig. 14 shows the final outcome with fabric alignment. With perfect alignment, the distance between the outer perimeters of the interlining fabric and shell fabric is about 2 mm, and the requirement for fusing purposes is to keep interlining fabric within the shell fabric outer perimeter. Our visual servoing is able to achieve this requirement 100% of the time when both shell and interlining fabric are picked up successfully.

VII. A Complete Demonstration of Fabric Fusing Process

With all components ready and environment set to about 50% relative humidity, the robot is able to complete the fabric fusing operations in the following steps:

Fig. 14: Aligned shell and interlining fabric is fed by the robot onto the conveyor belt at the end of each cycle.

Step 1: Jog to home configuration. (5 s)
Step 2: Jog to the top shell layer of the fabric. (5 s)
Step 3: Turn on voltage control to 9 kV and wait. (2 s)
Step 4: Jog to vision checking configuration. (7 s)
Step 5: Identify the fabric pose. If fabric is not found, throw an exception. (2 s)
Step 6: Bring the fabric centroid to the center of the region of interest and record the offset. (2 s)
Step 7: Place the fabric with offset. (5 s)
Step 8: Repeat Step 1 to Step 8 for the interlining fabric.
Step 9: Feed the combination to the fusing machine. (10 s)

Fig. 15 shows the snapshots of the robot performing each step in the fusing operation. The total time to complete one pair of shell and interlining fusing is about 66 seconds.

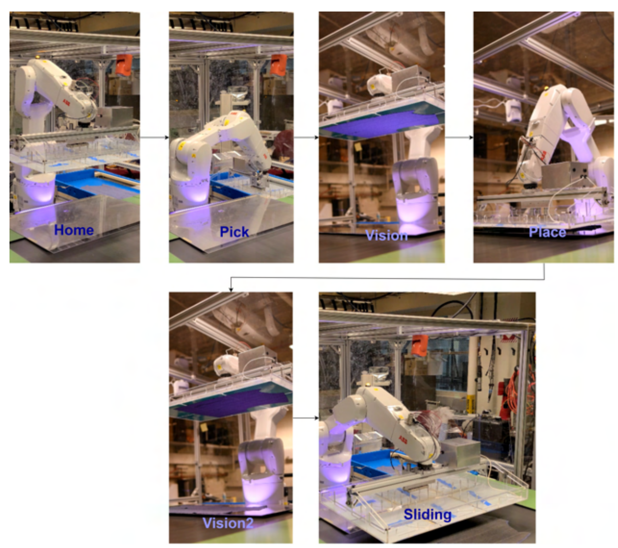

Fig. 15: Operation Steps: 1. Jog to home position; 2. Pick up the fabric; 3. Check the fabric pose on the gripper; 4. Place onto the station; 5. After performing the same steps for interlining fabric, check its pose as well; 6. Place the interlining with alignment and slide onto the fusing machine conveyor belt.

VIII. Conclusion and Future Work

This paper has presented a prototype robot garment handling system for fabric fusing using an electroadhesion gripper. The gripper is relative simple and inexpensive to construct. This system is able to perform the complete fusing operation on fabric pieces of different types, sizes and shapes. While electroadhesion for fabric handling is limited to a certain humidity range, as long as there is an enclosure around the working environment, the gripper is able to perform fabric fusing repeatedly and reliably. By using a higher voltage converter, the gripper may be able to pick up in a wider range of humidity. The output voltage may also be adapted to different types of fabrics under varying humidity conditions.

ACKNOWLEDGMENT

This research was supported by Advanced Robotics for Manufacturing Institute. Mechanical units and systems are developed by Manufacturing Innovation Center at Rensselaer with Glenn Saunders, William Lawler and Ken Myer. Interface Technologies LLC puts together a user interface for fusing operation with integration of Robot Raconteur. Thanks to Hickey Freeman for fabric supply and expertise on fusing process as well as on-site demonstration support.

REFERENCES

[1] D. Meike and L. Ribickis, "Energy efficient use of robotics in the automobile industry," in *2011 15th International Conference on Advanced Robotics (ICAR)*, 2011, pp. 507–511.

[2] K. Zhou *et al.*, "Mobile manipulator is coming to aerospace manufacturing industry," in *2014 IEEE International Symposium on Robotic and Sensors Environments (ROSE) Proceedings*, 2014, pp. 94–99.

[3] M. Hohn and C. Robl, "Qualification of standard industrial robots for micro-assembly," in *Proceedings 1999 IEEE International Conference on Robotics and Automation (Cat. No.99CH36288C)*, vol. 4, 1999, pp. 3085–3090 vol.4.

[4] H. Schuler, "Automation in chemical industry (automatisierung in der chemischen industrie)," *Automatisierungstechnik*, vol. 54, no. 8, pp. 363–371, 2006.

[5] M. Shibata, T. Ota, Y. Endo, and S. Hirai, "Handling of hemmed fabrics by a single-armed robot," in *2008 IEEE International Conference on Automation Science and Engineering*, 2008, pp. 882–887.

[6] S. Ku, J. Myeong, H.-Y. Kim, and Y.-L. Park, "Delicate fabric handling using a soft robotic gripper with embedded microneedles," *IEEE Robotics and Automation Letters*, vol. 5, no. 3, pp. 4852–4858, 2020.

[7] D. Hinwood, D. Herath, and R. Goecke, "Towards the design of a human-inspired gripper for textile manipulation," in *2020 IEEE 16th International Conference on Automation Science and Engineering (CASE)*, 2020, pp. 913–920.

[8] Z. Doulgeri and N. Fahantidis, "Picking up flexible pieces out of a bundle," *IEEE Robotics & Automation Magazine*, vol. 9, no. 2, pp. 9–19, 2002.

[9] K. Yamazaki and T. Abe, "A versatile end-effector for pick-and-release of fabric parts," *IEEE Robotics and Automation Letters*, vol. 6, no. 2, pp. 1431–1438, 2021.

[10] K. Manabe, X. Tong, and Y. Aiyama, "Single sheet separation method from piled fabrics using roller hand mechanism," in *2021 IEEE International Conference on Intelligence and Safety for Robotics (ISR)*, 2021, pp. 359–362.

[11] P. Koustoumpardis and N. Aspragathos, "A review of gripping devices for fabric handling," in *International Conference on Intelligent Manipulation and Grasping IMG04*, 07 2004.

[12] T. Nakamura and A. Yamamoto, "Modeling and control of electroadhesion force in dc voltage," *ROBOMECH Journal*, vol. 4, no. 1, p. 18, Jun 2017.

[13] P. Taylor, G. Monkman, and G. Taylor, "Electrostatic grippers for fabric handling," in *Proceedings. 1988 IEEE International Conference on Robotics and Automation*, 1988, pp. 431–433 vol.1.

[14] P. Taylor, A. Wilkinson, G. Taylor, M. Gunner, and G. Palmer, "Automated fabric handling problems and techniques," in *1990 IEEE International Conference on Systems Engineering*, 1990, pp. 367–370.

[15] G. J. Monkman, "Compliant robotic devices, and electroadhesion," *Robotica*, vol. 10, no. 2, p. 183–185, 1992.

[16] B. Sun and X. Zhang, "A new electrostatic gripper for flexible handling of fabrics in automated garment manufacturing," in *2019 IEEE 15th International Conference on Automation Science and Engineering (CASE)*, 2019, pp. 879–884.

[17] Grabit Inc, "Electroadhesion. it only looks like magic." Dec. 27, 2018. [Online]. Available: https://grabitinc.com/products

[18] H. Prahlad *et al.*, "Modular electroadhesive gripping system," U.S. Patent 20 160 318 190A1, Dec. 10, 2014.

[19] ——, "Methods and systems for electroadhesion-based manipulation and mechanical release in manufacturing," U.S. Patent 10 987 815B2, Apr. 27, 2017.

[20] J. Guo, T. Hovell, T. Bamber, J. Petzing, and L. Justham, "Symmetrical electroadhesives independent of different interfacial surface conditions," *Applied Physics Letters*, vol. 111, p. 221603, 12 2017.

[21] B. Behera, "Role of fabric properties in the clothing-manufacturing process," in *Garment Manufacturing Technology*, ser. Woodhead Publishing Series in Textiles, R. Nayak and R. Padhye, Eds. Woodhead Publishing, 2015, pp. 59–80.

[22] H. Prahlad *et al.*, "Electroadhesive robots—wall climbing robots enabled by a novel, robust, and electrically controllable adhesion technology," in *2008 IEEE International Conference on Robotics and Automation*, 2008, pp. 3028–3033.

[23] G. Hwang *et al.*, "Electroadhesion-based high-payload soft gripper with mechanically strengthened structure," *IEEE Transactions on Industrial Electronics*, vol. 69, no. 1, pp. 642–651, 2022.

[24] X. Liang *et al.*, "Delicate manipulations with compliant mechanism and electrostatic adhesion," in *2016 6th IEEE International Conference on Biomedical Robotics and Biomechatronics (BioRob)*, 2016, pp. 401–406.

[25] J. Guo *et al.*, "Optimization and experimental verification of coplanar interdigital electroadhesives," *Journal of Physics D: Applied Physics*, vol. 49, no. 41, p. 415304, sep 2016.

[26] J. Chestney and M. Sarbadi, "Dielectric selection for a robotic electrostatic gripping device," in *Seventh International Conference on Dielectric Materials, Measurements and Applications (Conf. Publ. No. 430)*, 1996, pp. 103–107.

[27] T. Bamber *et al.*, "Visualization methods for understanding the dynamic electroadhesion phenomenon," *Journal of Physics D: Applied Physics*, vol. 50, no. 20, p. 205304, apr 2017.

[28] Analog Devices, "Adalm1000 overview." Jan. 24, 2022. [Online]. Available: https://wiki.analog.com/university/tools/m1k

[29] J. Fessl, F. Mach, and J. Navrátil, "Design, fabrication and testing of electroadhesive interdigital electrodes," *Open Physics*, vol. 16, no. 1, pp. 430–434, 2018.

[30] The MathWorks, Inc., *MATLAB Partial Differential Equation Toolbox*, Natick, Massachusetts, United State, 2021. [Online]. Available: https://www.mathworks.com/products/pde.html

[31] J. D. Wason and J. T. Wen, "Robot raconteur: A communication architecture and library for robotic and automation systems," in *2011 IEEE International Conference on Automation Science and Engineering*, 2011, pp. 761–766.

[32] J. D. Wason, "Robot raconteur® version 0.8: An updated communication system for robotics, automation, building control, and the internet of things," in *2016 IEEE International Conference on Automation Science and Engineering (CASE)*, 2016, pp. 595–602.

[33] C. Cao, X. Sun, Y. Fang, Q.-H. Qin, A. Yu, and X.-Q. Feng, "Theoretical model and design of electroadhesive pad with interdigitated electrodes," *Materials & Design*, vol. 89, pp. 485–491, 2016.

[34] J. Guo *et al.*, "Experimental study of relationship between interfacial electroadhesive force and applied voltage for different substrate materials," *Applied Physics Letters*, vol. 110, no. 5, p. 051602, 2017.

[35] S. Lai, J. Zhang, Y. Yan, and H. Yu, "Optimization design strategy of electroadhesive devices with interdigital electrodes based on the multiparameters theoretical model," *Mathematical Problems in Engineering*, vol. 2021, p. 3737490, Sep 2021.

[36] G. Bradski, "The OpenCV Library," *Dr. Dobb's Journal of Software Tools*, 2000.

[37] J. Canny, "A computational approach to edge detection," *IEEE Transactions on Pattern Analysis and Machine Intelligence*, vol. PAMI-8, no. 6, pp. 679–698, 1986.